



Expandable pedicle screw may have better fixation than normal pedicle screw: preclinical investigation on instrumented L4-L5 vertebrae based on various physiological movements

Devismita Sanjay¹ · Jaideep Singh Bhardwaj¹ · Neeraj Kumar¹ · Souptick Chanda¹

Received: 14 February 2022 / Accepted: 24 June 2022 / Published online: 30 June 2022
© International Federation for Medical and Biological Engineering 2022, corrected publication 2022

Abstract

Lumbar spine fracture is typically treated by means of screw fixation, the primary aim of which is to reduce fracture by achieving bony union such that the spinal anatomy is restored. Pedicle screw fixation has certain advantages over conventional vertebral screws, e.g. 3-column fixation and improved surgical alignment. However, expandable pedicle screws have been reported to impart better anchorage as compared to conventional pedicle screws, both in case of healthy and osteoporotic bone. The clinical studies notwithstanding, there is a paucity of preclinical investigations on expandable pedicle screws used on lumbar vertebrae. By employing anatomically viable FE models, the present study intended to estimate stress–strain fields of a functional spinal unit (FSU) of intact L4-L5 vertebra and to further compare the same with FSUs instrumented with normal and expandable pedicle screws under different physiological loading condition. The various physiological loading regimes appeared to have significant influence on the overall load transfer in the L4-L5 vertebrae. The expandable pedicle screw predicted marginally improved anchorage as compared to the normal pedicle screws, with more contact area with the bone resulting in higher stresses (~1.6 MPa) and high strain at the contact sites. This is indicative of improved stability albeit having marginally greater risk of screw pullout. Greater area (15–80%) with peak stresses at the bone-screw interfaces also indicates lesser degree of stress shielding. Thus, stability aside, one may expect to have lower loosening issues too with the use of expandable pedicle screws.

Keywords Spine · Biomechanics · Finite element analysis · Pedicle screw · Fracture fixation

1 Introduction

A great number of the people across the globe suffer from mild to severe lower back pain, the onset of which can sometimes be postoperative. The lower back pain was reported as the second most symptomatic reason and overall fifth most common reason for all the physician visits [1]. The most common skeletal complaint of the spine and hip for elderly people is osteoporosis with mortality rates ranging from 10 to 20% [2]. These osteoporotic fractures also cause extensive pain and, in certain cases, disability, depression, and increased dependency leading to diminished quality of life

[2]. Each year, nearly 700,000 patients suffer from spinal fractures known as vertebral compression fractures. Lumbar surgeries are predominantly performed 3 times more for patients older than 60 years than younger ones [3, 4]. It may be noted here that the lumbar spine helps in transferring the weight to the pelvis and allows different bodily movements during day-to-day activities [5–7].

During the pre-renaissance era and also during the two world wars, different surgical techniques were tried by physicians to treat lumbar spine fracture. Vertebral and pedicle screw fixations were introduced in the 1940s and became popular ever since among spine surgeons [8]. The first case of vertebral screw fixation started way back in 1944. However, the use of pedicle screw was well documented since the 1970s by Roy-Camille [8]. The primary aim of the surgeons was to reduce fracture by achieving bony union, such that the spinal anatomy is restored while delivering stability to the posterior spinal devices [9].

✉ Souptick Chanda
csouptick@iitg.ac.in

¹ Department of Biosciences and Bioengineering, Indian Institute of Technology Guwahati, Guwahati 781 039, Assam, India

Pedicle screws offer stability of the posterior side with rigid bony fixation by connecting the fractured bones [10]. The chief advantages of pedicle screws over conventional bone screws are that they provide 3-column fixation, assist in instrumentation of short segment, and also maintain desired alignment [11, 12]. The success rate of pedicle screw fixation was found to be more than 80% in a 10-year follow-up study [13]. In case of posterior fixation, however, it was estimated that pedicle screw was the feeblest link [14, 15]. The primary failure of pedicle screw was found to occur either due to screw loosening or screw root breakage [10, 14, 16–21]. Loosening of pedicle screw can be ascribed to increased load sharing, high stress concentration caused by bending, frequent loading–unloading, and prolonged bone fusion [22–24]. Earlier studies suggested that bone mineral density, insertion technique, and screw dimensions act as necessary factors for screw stability [20, 25]. Patients with osteoporosis have low bone mineral density and thus have lower pullout strength at the fixation points [3, 26–28]. The inferior bone quality in osteoporotic spine may pose a challenge for surgeons to operate as it may lead to complications in the neural structures owing to failure at bone–screw interface [29–31]. Earlier studies suggested that sagittal imbalance was a primary pathogenic cause of lower back pain and its correction was essential for degenerative spinal deformity [28, 32].

Expandable pedicle screws, on the other hand, have many advantages over traditional pedicle screws because of its capacity for better anchorage. Earlier studies indicated that expandable pedicle screws provide better fixation due to greater bone contact without any increase in diameter or screw length [33]. The use of expandable pedicle screws resulted in an increase of around 30% and 50% in pullout strength in case of healthy and osteoporotic bone, respectively, as compared to conventional pedicle screws [34]. This suggests that expandable pedicle screws tend to provide superior fixation strength in case of compromised bone. For osteoporotic patients, expandable pedicle screw provides less complications, quick and surgically satisfactory post-operative effect, short operation time, and less intraoperative bleeding [35]. Breakage of expandable pedicle screw occurred for around 2.8% patients and 2.6% in total number of screws that were placed [33]. The clinical studies notwithstanding, there is, of course, a paucity of preclinical investigations on expandable pedicle screws used on lumbar vertebrae. Therefore, more rigorous investigations are warranted to evaluate its performance, and to further ascertain its competitive edge over other techniques, if any.

Over the last few decades, finite element (FE) analysis has attained much popularity as a preclinical tool in orthopaedics and courtesy its non-invasive nature, novel designs of implants have been studied *in silico* [36–41]. It has been used extensively to solve many biomechanical problems

owing primarily to low financial and computational cost, as well as high precision simulation [38, 42]. It further reduces the complexity of clinical or *in vitro* tests. In studies involving lumbar spine biomechanics, FE helped gain insights at crucial sites, e.g. bone–screw interfaces under different physiological conditions of spinal loads [43–46]. Thus, evaluation of different spinal implants and development of subject-specific implants have been attempted using FE [40, 42–45, 47, 48]. Nonetheless, a realistic FE model of the spinal osteotomies is paramount in this regard, which may successfully allude to more detailed preclinical insights and thereby help clinicians choose the right implant [40, 49, 50].

It was estimated that failure was greatest (33% for single level fusion) at L4–L5 level among all vertebral screw fixation [8]. By employing anatomically viable FE models, the present study intended to estimate stress–strain fields of a functional spinal unit (FSU) of intact L4–L5 vertebra and to further compare the same with FSUs instrumented with normal and expandable pedicle screws under various physiological loading conditions. Stress and strain results for intact and implanted models, corresponding to various physiological movements, were derived and subsequently used to compare between the normal and expandable pedicle screws. It is hypothesized hereto that expandable pedicle screw may result in improved stability and more anatomic load transfer as opposed to normal pedicle screw.

2 Materials and methods

An elaborate description of materials and method starting from the development of virtual osteotomies until the *in silico* biomechanical investigations has been laid out piecemeal under the following subcategories.

2.1 Development of the intact model

Figure 1a shows the CAD model of intact L4–L5 vertebrae. All different parts of the FSU, i.e. the intact L4–L5 vertebrae, are illustrated in Fig. 2. The virtual FSU was generated using the CAD models of L4 (model #3902) and L5 (model #3901) vertebrae, procured from the manufacturer (Sawbones, Europe AB, Malmo, Sweden). The FSU was anatomically placed using Rhinoceros CAD software (Rhinoceros v7.0, Robert McNeel & Associates Seattle, USA), and modifications such as the Boolean operations were carried out for digital separation of cortical and cancellous bone. The average thickness of the cortical bone was considered to be 1.0 mm [51, 52]. Thereafter, annulus fibrosus and nucleus pulposus comprising the intervertebral disc (IVD) were curated. Around 43% of the whole disc volume was occupied by nucleus pulposus [53]. The bony endplates and cartilaginous endplates were given a thickness of 0.5 mm

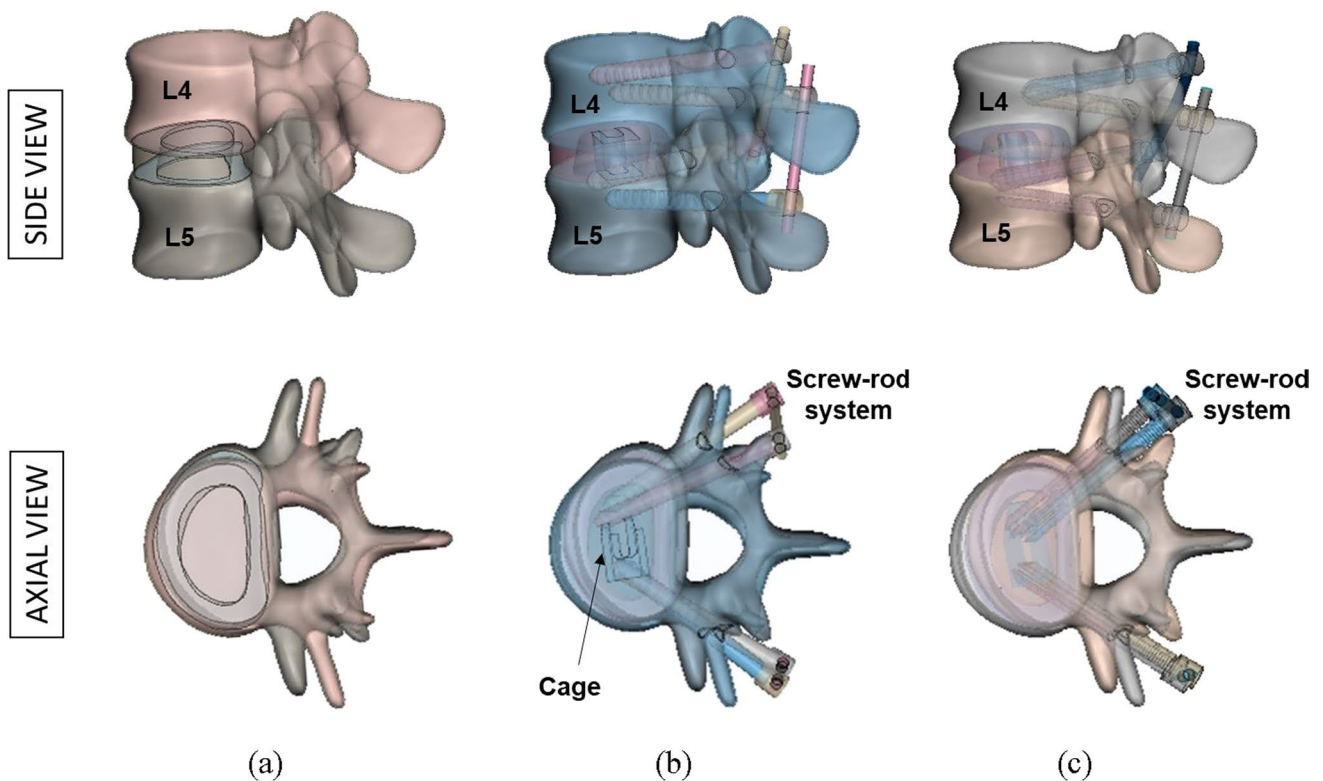


Fig. 1 3D CAD models the L4-L5 FSU: (a) intact, (b) implanted with normal pedicle screw, and (c) implanted with expandable pedicle screw

[40]. Further, the facet cartilage was developed based on an initial gap of 0.1 mm [40].

2.2 Development of the implanted models

Figure 1b and Fig. 1c demonstrate the CAD models of implanted L4-L5 vertebrae with normal pedicle screw and expandable pedicle screw, respectively. Lumbar loading reconstruction is generally carried out by posterior pedicle screw-rod fixation because of great loading conditions [54]. Various parts of implanted L4-L5 vertebrae are displayed in Fig. 3. Transformational lumbar interbody fusion (TLIF) has been reported to be a popular choice for the treatment of degenerated lumbar spine and against premature pedicle screw loosening [55, 56]. As such, one-sided total facetectomy was performed to virtually place the TLIF cage (Ardis™, Zimmer Biomet, Warsaw, IN, USA, 26 × 11 × 12 mm) inside the FSU (Fig. 3). It was estimated that enlarged screw diameter that optimally fits the pedicle leads to a better screw stability [20, 21]. Cylindrical screws of 60.0 mm length (body length: 26.5 mm; thread length: 33.5 mm), 6.0 mm shaft diameter, and 3.0 mm pitch having triangular threads (angles: 90°, 36.7°, and 53.3°) were considered for both normal and expandable pedicle models (Fig. 3). The normal pedicle screw design was based on EXPEDIUM 5.5 system (DepuySynthes Spine, Inc.,

Raynham, MA), and expandable pedicle screw design was adopted from Tai et al. (2015) [57]. The expandable pedicle screw had an extension of around 2.0 mm in diameter after the expansion [12]. For all the implanted models, the removal of nucleus pulposus, cartilaginous endplates, and left facet cartilage was performed as per the surgical guidelines. Two rods, each 50.0 mm long having diameter 4.0 mm, were inserted through screw head for securing the implants properly. It is extremely essential for the surgeons to place the pedicle screws properly in order to have correct placement as well as to minimize the risk of revision surgery [58]. The screws and the rods were inserted into the vertebrae following proper angulation guidelines after consulting with an experienced orthopaedic registrar (Max Hospital, Mohali, India).

2.3 FE model generation and analysis

The FE models of both intact and implanted L4-L5 vertebra were generated using HyperMesh 2021.1 (Altair Engineering Inc., Troy, MI, USA) (Figs. 2 and 3). A mesh convergence study of intact L4-L5 FE model was performed in order to optimize the element size for a trade-off between accuracy and solution speed. Three FE models of different element sizes were generated to estimate the dependency on mesh density. Equivalent (von-Mises) stress of

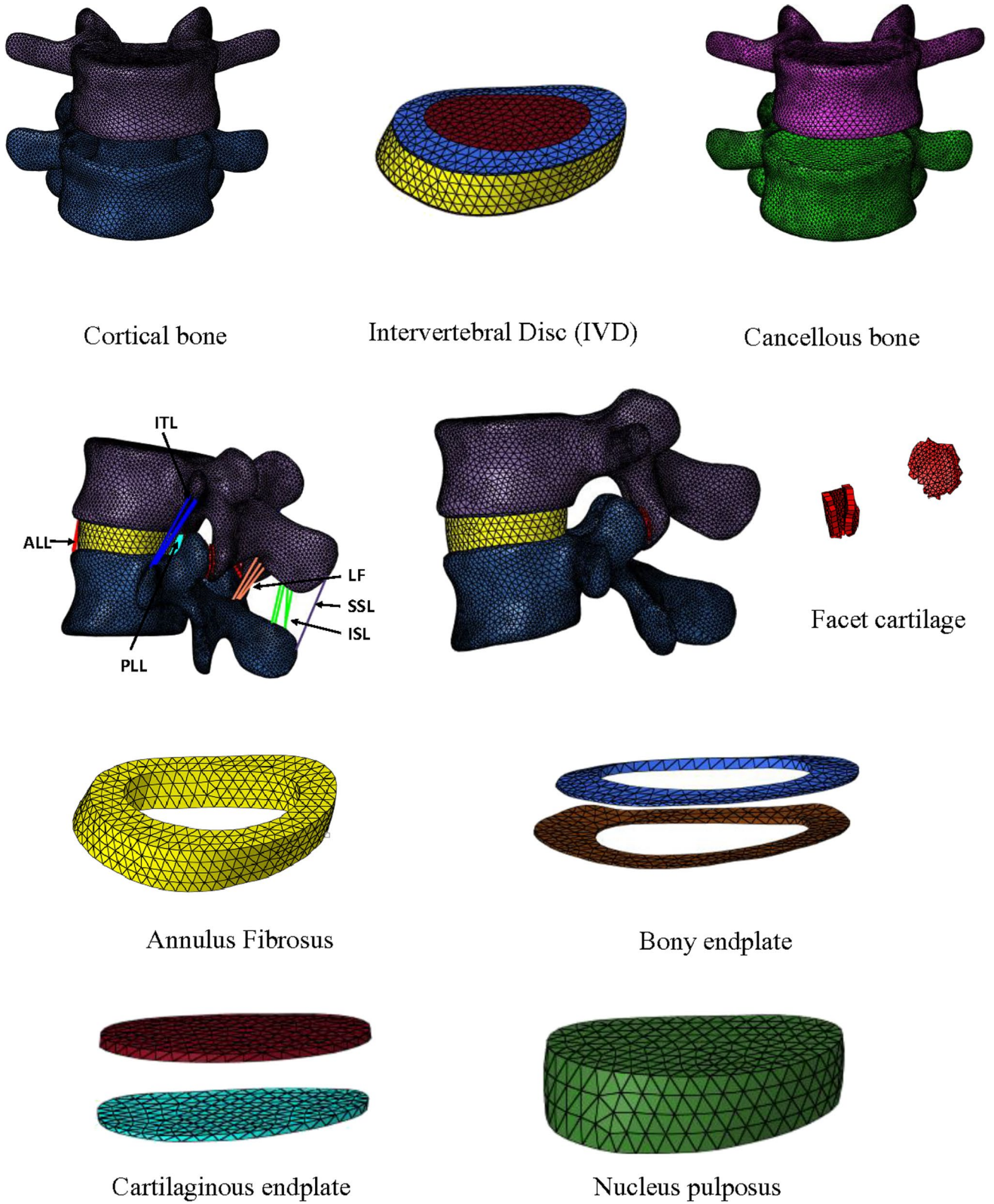


Fig. 2 The curated models of different parts of an intact L4-L5 FSU

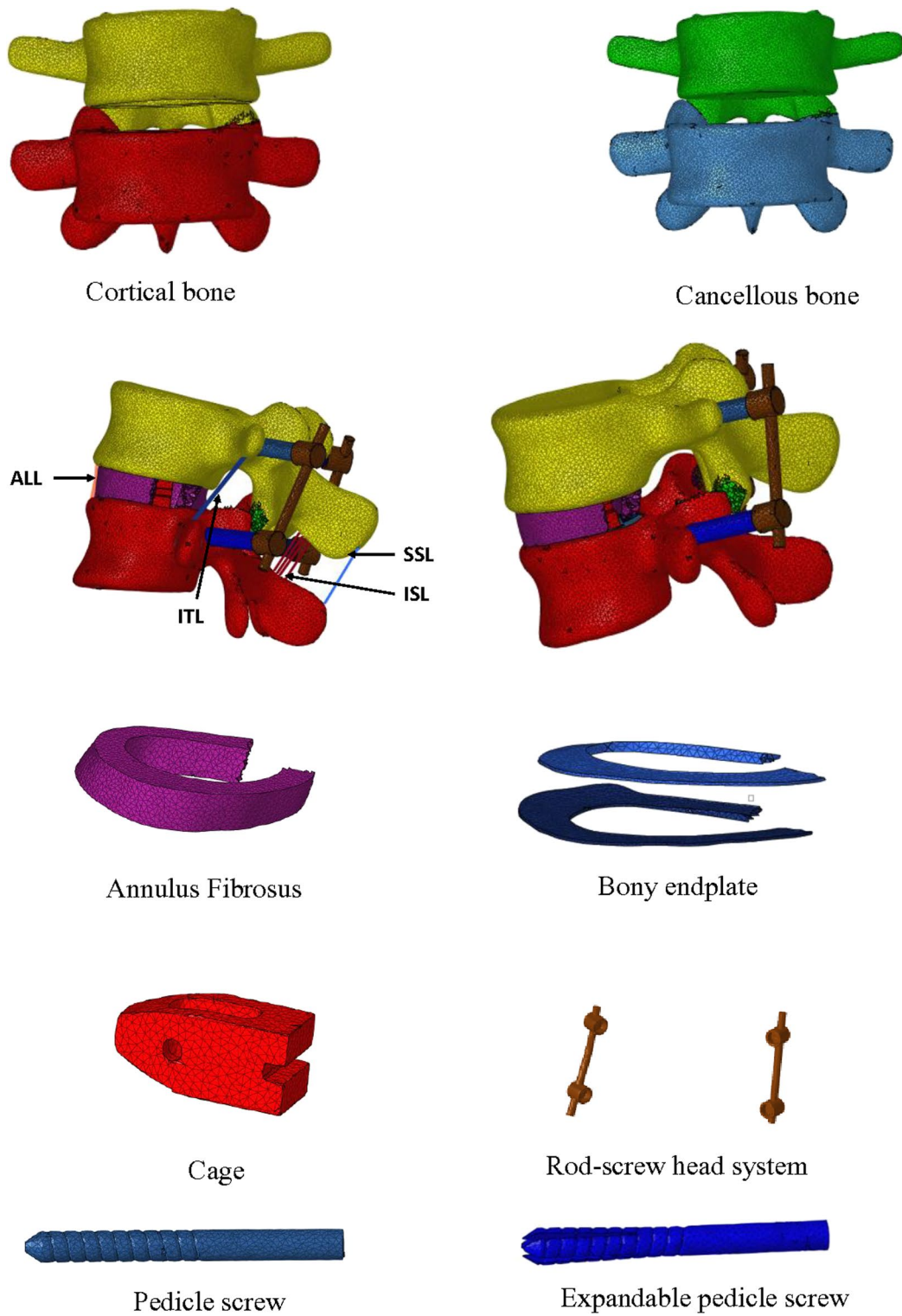


Fig. 3 The curated models representing different parts of the two implanted L4-L5 FSUs

cortical and cancellous bone under pure compression was chosen for mesh convergence study. The von-Mises stress varied between 4 and 6% for the first two FE models, whereas ~1–2% deviation was observed for second and

third model [41]. Thus, the second model, which consisted of 647,837 elements in the entire implant-bone assembly having maximum element size of 2.5 mm, was selected for further analyses. The solid models of bones and the

implants were discretized into 4-noded unstructured tetrahedral mesh, wherein the average edge length was considered to be ~ 1.0 mm (Fig. 2 and Fig. 3). However, the six ligaments, namely, anterior longitudinal ligament (ALL), posterior longitudinal ligament (PLL), ligamentum flavum (LF), intertransverse ligament (ITL), interspinous ligament (ISL), and supraspinous ligament (ISL), were modelled using 1D tension-only spring elements, termed as CGAP elements (Figs. 2 and 4a). These elements can mimic the soft tissue properties since they impart stiffness only under tension [41], whereas in compression, the stiffness becomes zero. Both LF and PLL were removed, however, for all implanted models as per surgical guidelines (Figs. 3 and 4b and c).

All analyses were performed using ‘OptiStruct’ solver of HyperMesh 2021.1. Considering stiffness as a function of displacement, the nonlinear analysis was executed by following piecewise linearity so that load was split into small increments. Thus, the stiffness matrix was restructured after each increment of applied load. Newton–Raphson method was used to solve the equations iteratively [59].

The contact analysis was solved using augmented Lagrangian method, where L4 cartilage was considered as slave (contact) and L5 cartilage as master body (target) in the contact pair [6]. It is important to note that surface-to-surface contact elements were used (coefficient

of friction, $\mu=0.2$) [60] on both left and right side of the facet cartilage interface of L4-L5 vertebrae.

2.4 Material properties

The material properties of cortical bone, cancellous bone, and end plates were assumed to be linear, elastic, and isotropic [17, 61]. For nucleus pulposus, low elastic modulus ($E=0.1$ MPa) was applied with the aim of simulating incompressible fluid-like behaviour [62]. The implant material was considered to be titanium alloy (Ti-alloy) having Young’s modulus of 110 GPa and Poisson’s ratio of 0.3. All material properties are tabulated in Table 1.

The lengths of the ligaments were obtained from data available in the literature [5]. The stiffness values of the ligaments, as shown in Table 2, are estimated based on the length, anatomical cross section, and Young’s moduli [51, 62, 63]. For calculating the ligament stiffness, the axial stiffness formula, i.e. $K=AE/L$ was used, where K is the geometric stiffness, A is the cross-sectional area, E is the Young’s modulus, and L is the length of the ligament. The calculated values were found to corroborate well with the literature [5].

2.5 Loading and boundary conditions

The analyses were performed for five loading conditions, i.e. compression, flexion, extension, lateral bending, and torsion, as described in our earlier work [6], and all load

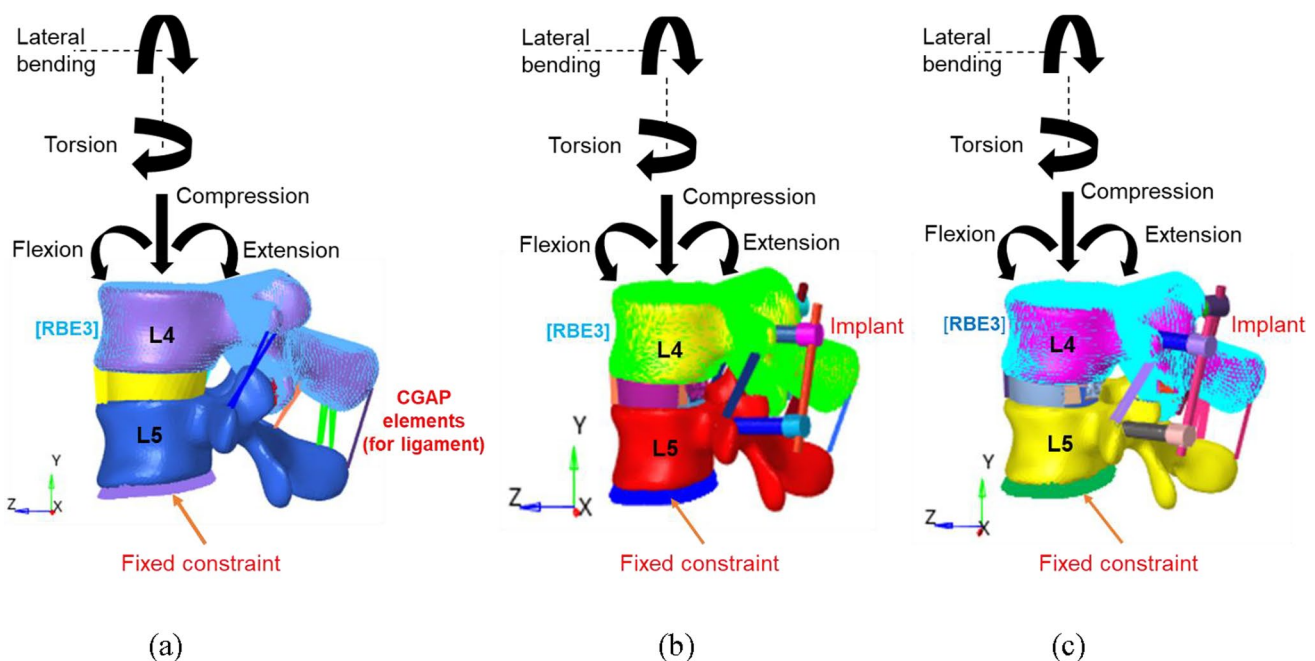


Fig. 4 The various physiological loading and boundary conditions for (a) intact FE model, (b) implanted FE model for normal pedicle screw, and (c) implanted FE model for expandable pedicle screw.

‘RBE3’ denotes the rigid body element surrounding the L4 vertebra, whereas ‘CGAP’ elements were defined to simulate ligament properties

Table 1 Material properties corresponding to various components of the FSU

Components	Young’s modulus (MPa)	Poisson’s ratio	References
Cortical bone	12,000	0.3	Li et al. (2014) [9], Goel et al. (2007) [48]
Cancellous bone	100	0.3	Li et al. (2014) [9], Goel et al. (2007) [48]
Bony endplate	1200	0.29	Li et al. (2014) [9]
Cartilaginous endplate	23.8	0.4	Xu et al. (2016) [47]
Nucleus pulposus	0.1	0.49	Li et al. (2014) [9]
Annulus fibrosus	9	0.4	Li et al. (2014) [9]
Cage	110,000	0.3	Su et al. (2021) [31]
Pedicle screw	110,000	0.3	Wong et al. (2022) [61]
Ti rod	110,000	0.3	Wong et al. (2022) [61]

Table 2 Ligament properties

Ligaments	Stiffness (N/mm)
Anterior longitudinal	45.20
Posterior longitudinal	26.49
Flavum	43.71
Intertransverse	2.77
Interspinous	35.50
Supraspinous	12.72

values loosely correspond to the body weight of an adult person [6, 64]. A rigid body element (RBE3) was created for the application of load (Fig. 4a, b, and c). Roughly at the centre of top surface of L4 cortical bone, a ‘dependent’ node was selected, whereas all surface nodes of L4 cortical bone were selected as ‘independent’ nodes. The loads were applied at the central node of RBE3 and calculated based on the weighted average of motions for all the surface nodes of L4 cortical (Fig. 4) [6]. Thus, the loads were assumed to be acting through the centre of gravity of L4. For axial compression loading condition, a load of 500 N was applied vertically downward. However, for flexion, extension, lateral bending, and torsion, a 10 N-m moment plus an axial load of 500 N acted upon simultaneously on the FSU [6, 64, 65]. For the purpose of FE analysis, all interfaces in the FSU—intact and implanted—were assumed to be bonded under all conditions [6]. All the bottom surface nodes of L5 cortical of the FSU were constrained for all six degrees of freedom [6, 51, 55] (Fig. 4).

3 Result

3.1 L4-L5 FSU: model validation based on ROM

The validation of the L4-L5 FSU (intact model) was performed by comparing results of range of motion (ROM) vis-à-vis various loading regimes, both based on experimental

data [65] as well as FE analysis reported erstwhile [64] (Fig. 5). Under axial compression, the experimental study by [65] reported a maximum relative displacement of 0.38 mm, whereas the same was predicted to be 0.88 mm in the FE study [64]. In our study, the predicted linear displacement (in mm) under axial compression (Fig. 5e) was found to lie midway between the earlier two findings (~0.65 mm). In case of flexion, extension, torsion, and lateral bending, the ROM (calculated as angular displacements having unit in degrees) versus load graphs were found to follow similar trends and to agree reasonably with the literature (Fig. 5a–d). All ROM values (in degrees) are shown in Table 3 for direct comparison with data from the literature.

3.2 ROM of the implanted models

ROM was reported to be the highest in the intact spine [66], and hence, for all ROM deviations in the implanted models, intact spine was considered as the reference (i.e. 100%). Considerable reductions in ROM were predicted for the implanted models while subjected to different loading regimes. For normal pedicle screw models, the reductions were found to be 74%, 75%, 63%, and 50% under flexion, extension, torsion, and lateral bending, respectively. In case of expandable pedicle screws, the respective reductions were predicted in the order of 75%, 62%, 48%, and 39%.

3.3 Stress (von-Mises) for cortical and cancellous bone

The equivalent (von-Mises) stress contours for the cortical and cancellous bone of L4-L5 vertebrae, subjected to the five physiological loading regimes, are presented in Fig. 6 and Fig. 7, respectively. Figure 8 depicts the stress contour for cancellous bone in sectional view. While subjected to torsion, high stress magnitudes in the order of ~50 MPa (Fig. 6a) and ~1.6 MPa (Fig. 7a) were predicted in cortical and cancellous bone, respectively, in case of intact FSU. Under extension, peak stress was found to be close

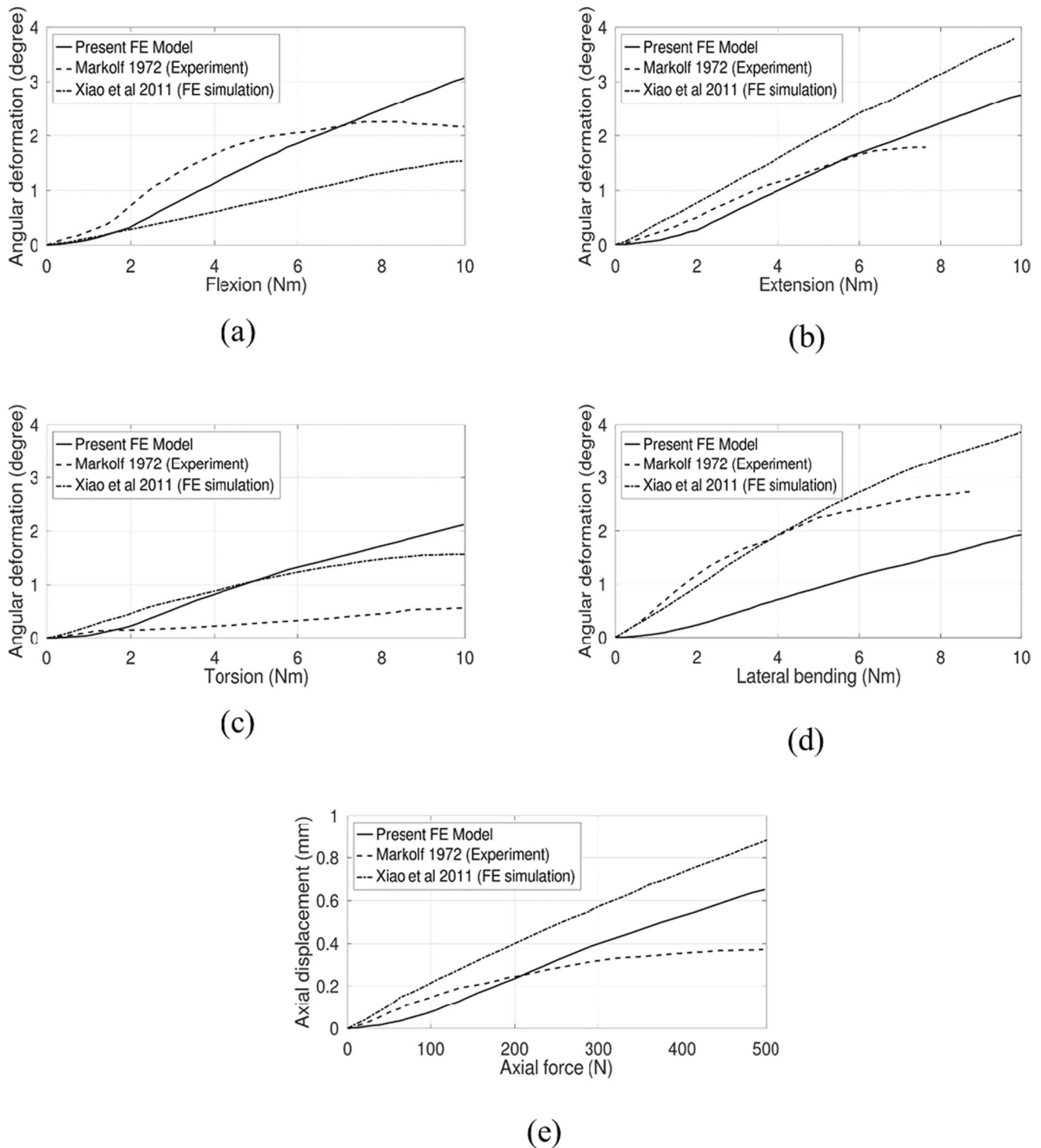


Fig. 5 Comparison of ROM values of the current intact FE model with those obtained from the literature: (a) flexion, (b) extension, (c) torsion, (d) lateral bending, and (e) axial compression

to 50 MPa for cortical bone albeit at a localized region, whereas for cancellous bone, the peak stress was ~ 0.9 MPa. Under compression loading, however, the peak stresses were predicted to be the least, i.e. ~ 15 MPa (Fig. 6a) for cortical bone and ~ 0.7 MPa (Fig. 7a) for cancellous bone. The peak

stresses were found towards the posterior side of the FSU, except for lateral bending condition where the peak stress was observed towards the anterior side (Figs. 6a and 7a).

For the implanted vertebrae with normal pedicle screw, peak stresses of ~ 10 MPa for cortical and ~ 1.6 MPa for

Table 3 ROM (in degrees) of intact model during different physiological movements

	Flexion	Extension	Torsion	Lateral bending
<i>Present study</i>	3.0	2.7	2.1	1.9
<i>Talukdar et al. (2021) [40]</i>	3.2	3.1	2.3	3.1
<i>Xiao et al. (2011) [65]</i>	1.6	3.7	3.8	1.6
<i>Zhong et al. (2006) [68]</i>	2.4	2.3	3.2	3.7
<i>Chen et al. (2001) [69]</i>	4.5	3.9	2.0	2.0
<i>Yamamoto et al. (1989) [67]</i>	7.1	4.0	2.4	3.8

cancellous bone were predicted under compression, whereas the same were found to be ~ 50 MPa and 1.6 MPa, respectively, under extension (Fig. 6b and Fig. 7b). These higher stress magnitudes were found at the site of screw insertion for cortical bone and near the cage insertion area for cancellous bone. Under lateral bending, the peak stress area was found to be shifted towards the anterior side, more predominantly on L5 vertebra as compared to L4 vertebra (Figs. 6b and 7b).

In case of expandable pedicle screw model, the highest stress of ~ 1.6 MPa (Fig. 7c) for cancellous bone was predicted under all the loading scenarios near the cage insertion area. However, scattered regions of comparable stress concentration were also predicted at the posterior side of L4 vertebra. In cortical bone, peak stresses (~ 50 MPa) (Fig. 6c) were predicted near posterior top side of L5 vertebra and also near screw insertion area under extension. Relatively moderate peak stress values (~ 45 MPa) were found under torsion and lateral bending for cortical bone towards the anterior side of L5 vertebra. The least amount of peak stress values for both cortical (~ 30 MPa) and cancellous bone (~ 1.4 MPa) were found under compression (Figs. 6c and 7c).

3.4 Strain (von-Mises) for cortical and cancellous bone

The equivalent (von-Mises) strain contour for L4-L5 vertebra for both cortical bone (Fig. 9) and cancellous bone (Fig. 10) under five physiological loading conditions is presented. In case of intact FSU, peak strains of ~ 0.0015 (Fig. 9a) for cortical bone and ~ 0.005 (Fig. 10a) for cancellous bone were observed under torsion. Under compression loading, peak strain was found to be below 0.0005 for cortical bone (Fig. 9a) and under 0.003 (Fig. 10a) for cancellous bone in case of intact FSU. The peak strain for both cortical bone (Fig. 9a) and cancellous bone (Fig. 10a) was found near posterior side of the FSU under all loading conditions except for lateral bending.

For implanted L4-L5 vertebra with normal pedicle screw, peak strains of ~ 0.002 for cortical bone (Fig. 9b) and ~ 0.007 for cancellous bone (Fig. 10b) were observed. However, peak strains were predicted to prevail over relatively greater area while subjected to extension load (Figs. 9b and 10b). High strain area was predominantly found near screw insertion in case of cortical bone and near cage area for cancellous bone. For various loading cases, the peak strain was estimated to be more in L5 than L4 vertebra (Figs. 9b and 10b). Following trends from stress results, the peak strain area corresponding to expandable pedicle screws was found to be greater than that in normal pedicle screws (Figs. 9c and 10c).

3.5 Stress-strain behaviour of the IVD

Figure 11 represents the stress-strain curve for the IVD obtained under compression load for the intact FSU. IVD for intact and implanted models exhibit similar stress-strain characteristics as shown in Fig. 11. The maximum stress in the intact IVD was predicted to be 1.53 MPa corresponding to a strain value of 0.157. However, compared to the intact model, the maximum stresses in IVD for the implanted cases were found to be less (0.9 MPa and 0.5 MPa, respectively, for normal and expandable pedicled spine).

4 Discussion

The present study was aimed at carrying out a comparative analysis between normal pedicle screw and expandable pedicle screw with regard to their postoperative performance in lumbar vertebrae fixation. The implanted models were preclinically assessed vis-à-vis intact L4-L5 FSU under different physiological movements to gain insights into their biomechanical behaviour. This study is specifically helpful to understand any deviation in load transfer and stability occurring in the implanted bones with reference to the intact condition.

Previous studies suggested that proper loading and boundary condition play a significant role for biomechanical analysis in lumbar FSU [40]. The validation of the model was done considering the ROM under various loading conditions [64, 65]. The loading conditions were obtained from the available literatures [51, 64, 65]. Axial compression loading of 500 N was applied vertically downward at the top surface of cortical of L4. This type of loading may arise while standing. In all the other four loading conditions, the axial force of 500 N was considered together with the moment of 10 N-m. The magnitude of moment was kept same in all four cases of physiological movements though it differed in direction depending on the load case (Fig. 4).

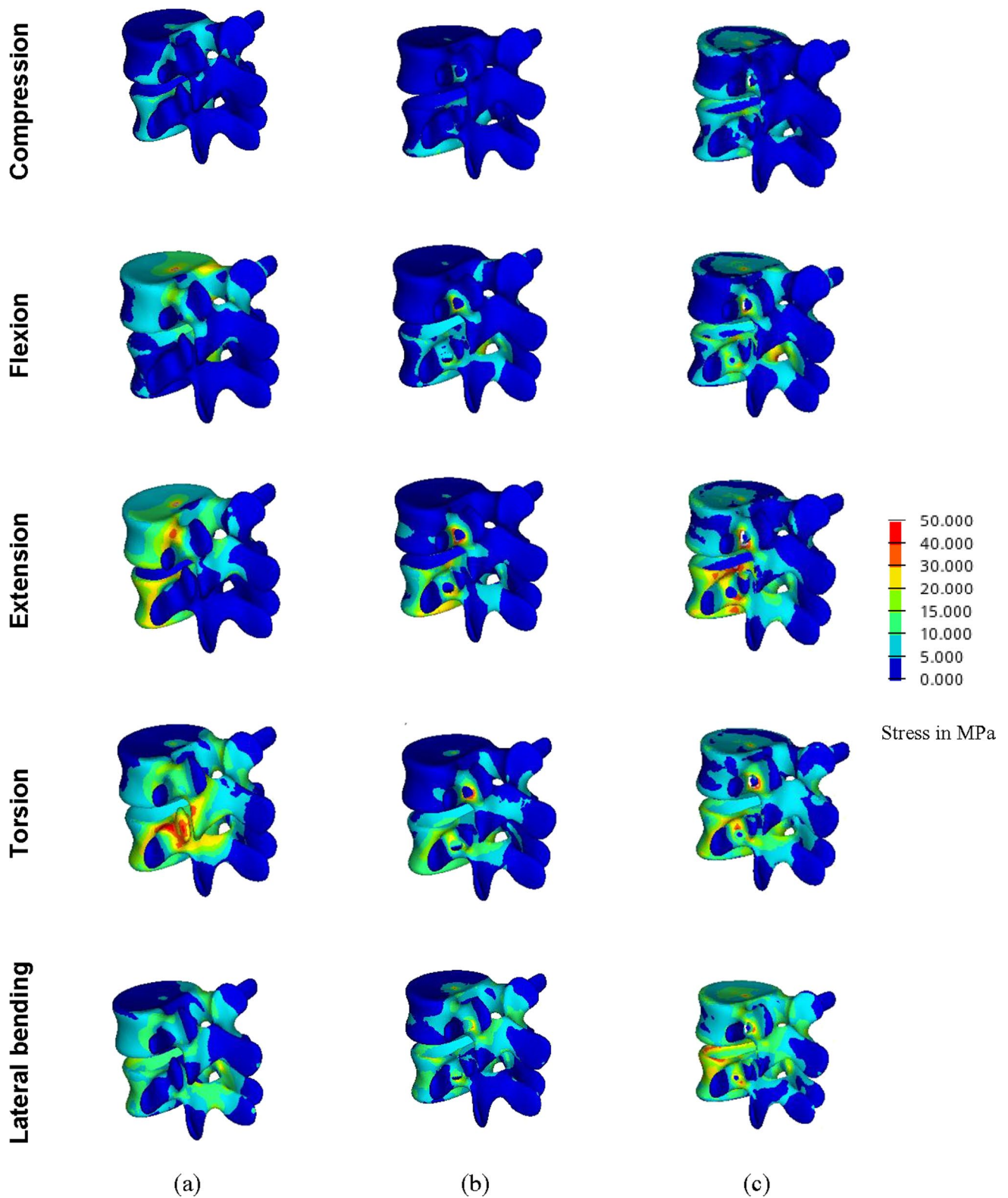


Fig. 6 Von-Mises stress contours (in MPa) in cortical bone for (a) intact FSU and FSUs corresponding to (b) normal and (c) expandable pedicle screw, respectively

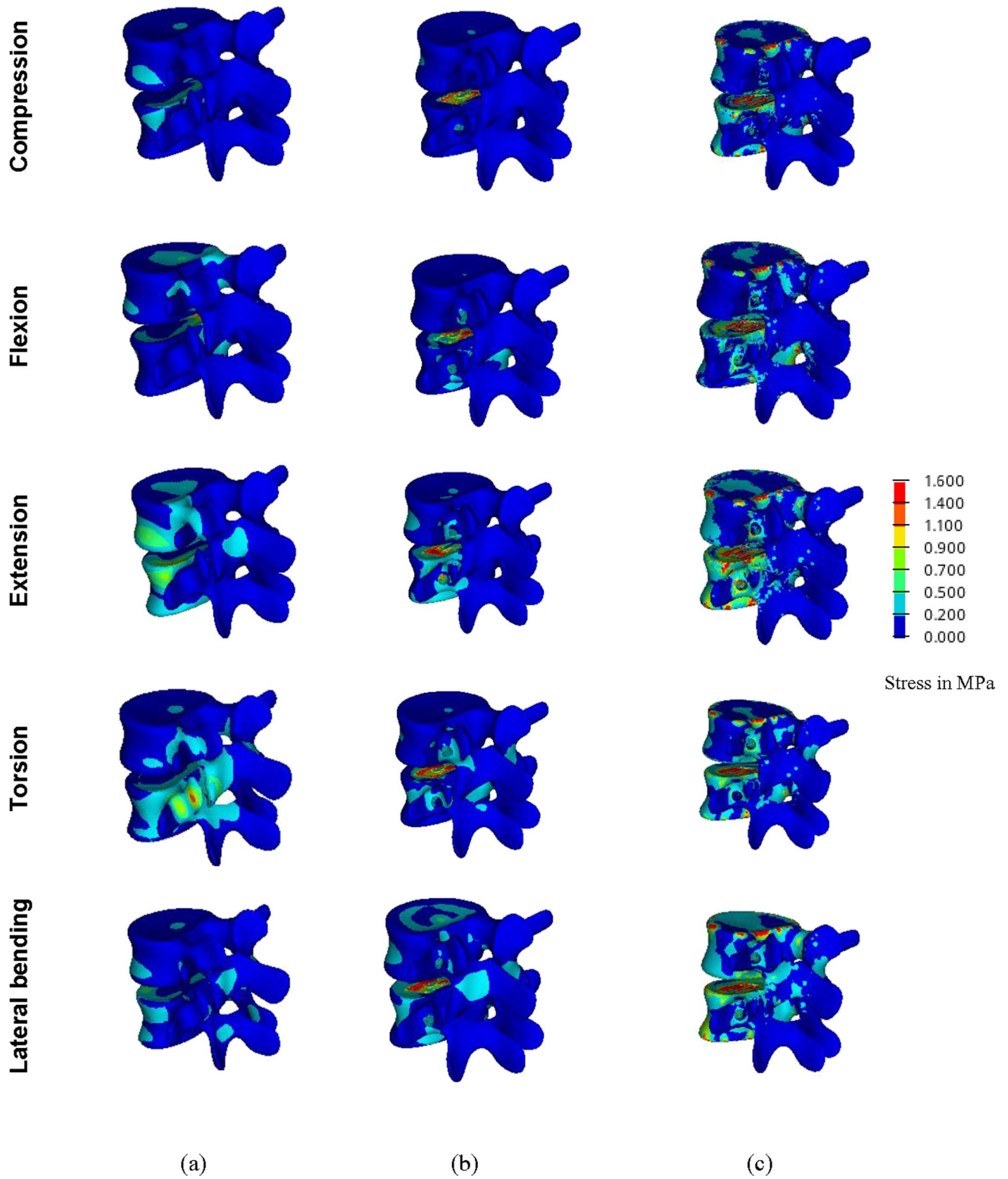


Fig. 7 Von-Mises stress contours (in MPa) in cancellous bone for (a) intact FSU and FSUs corresponding to (b) normal and (c) expandable pedicle screw, respectively

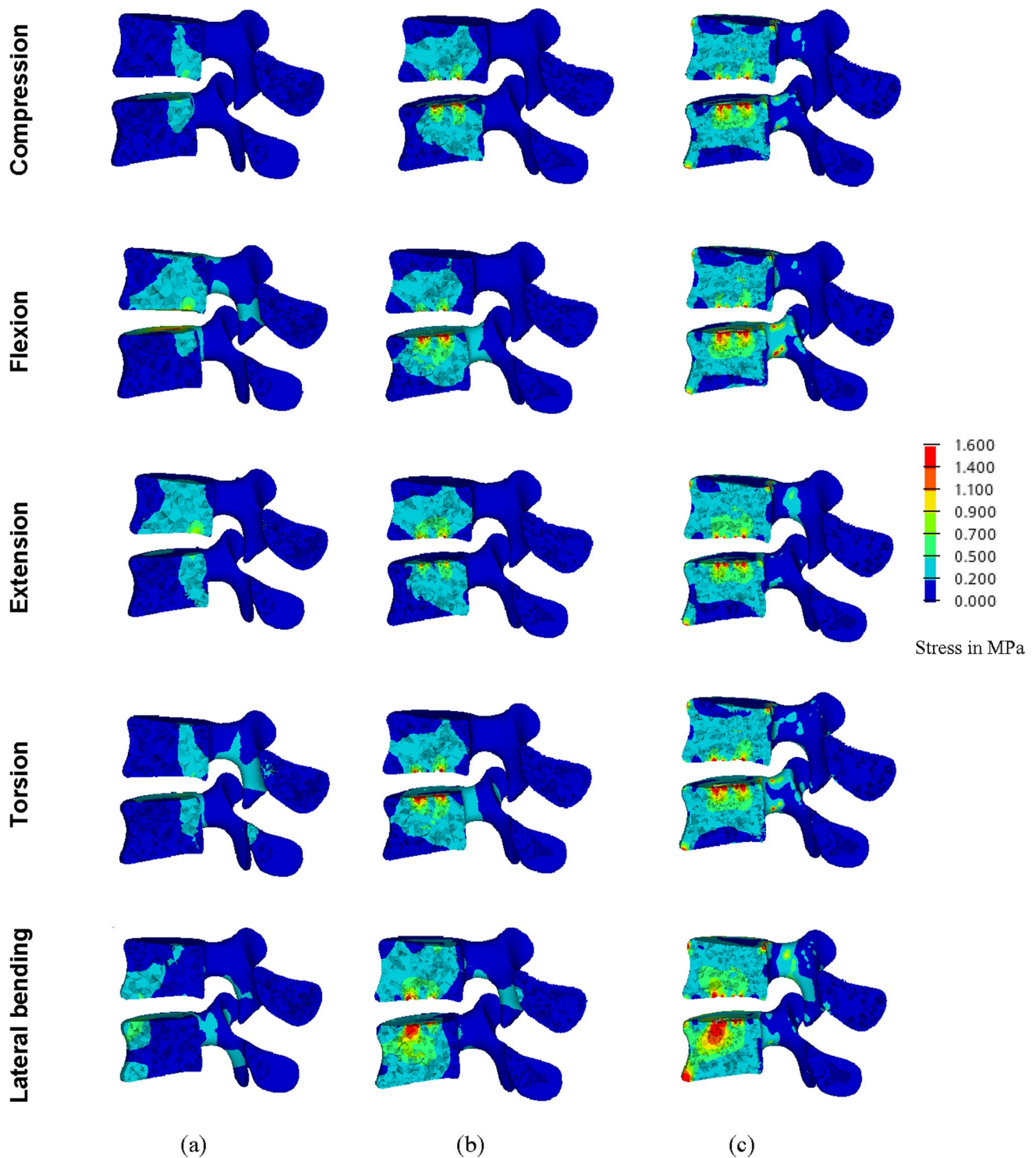


Fig. 8 Von-Mises stress contours (in MPa) in cancellous bone (*sectional view*) for (a) intact FSU and FSUs corresponding to (b) normal and (c) expandable pedicle screw, respectively

The ROM of the intact L4-L5 model was validated with previous studies and found to be in good agreement with earlier reported literature [40, 64, 67–69]. Implantation led to a discernible reduction in ROM for most cases

[40]. The reduction in ROM was found to be the highest in case of flexion–extension, and the least in case of lateral bending. The reductions in ROM were lesser in case of expandable pedicle screw model as compared to those

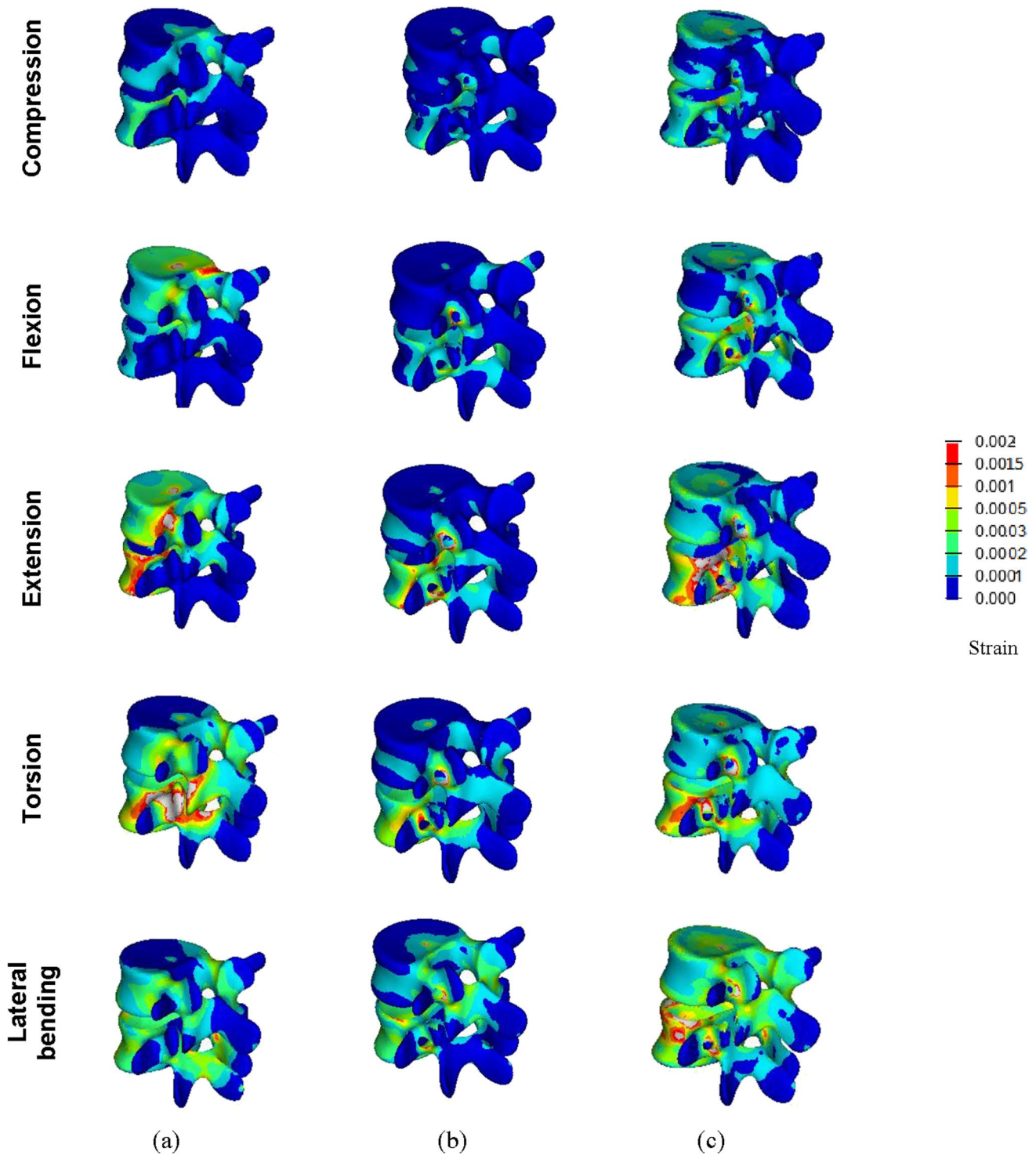


Fig. 9 Von-Mises strain contours in cortical bone for (a) intact FSU and FSUs corresponding to (b) normal and (c) expandable pedicle screw, respectively

for normal pedicle screw. Furthermore, the ROM values for the former were found to be relatively identical to the intact case, suggestive of a more anatomic functioning of the implanted FSU.

Application of different loading and boundary conditions used in FE models was found to have notable influence on stress variations in lumbar vertebrae. Earlier studies with implants (pedicle screw) [59] reported stress concentration

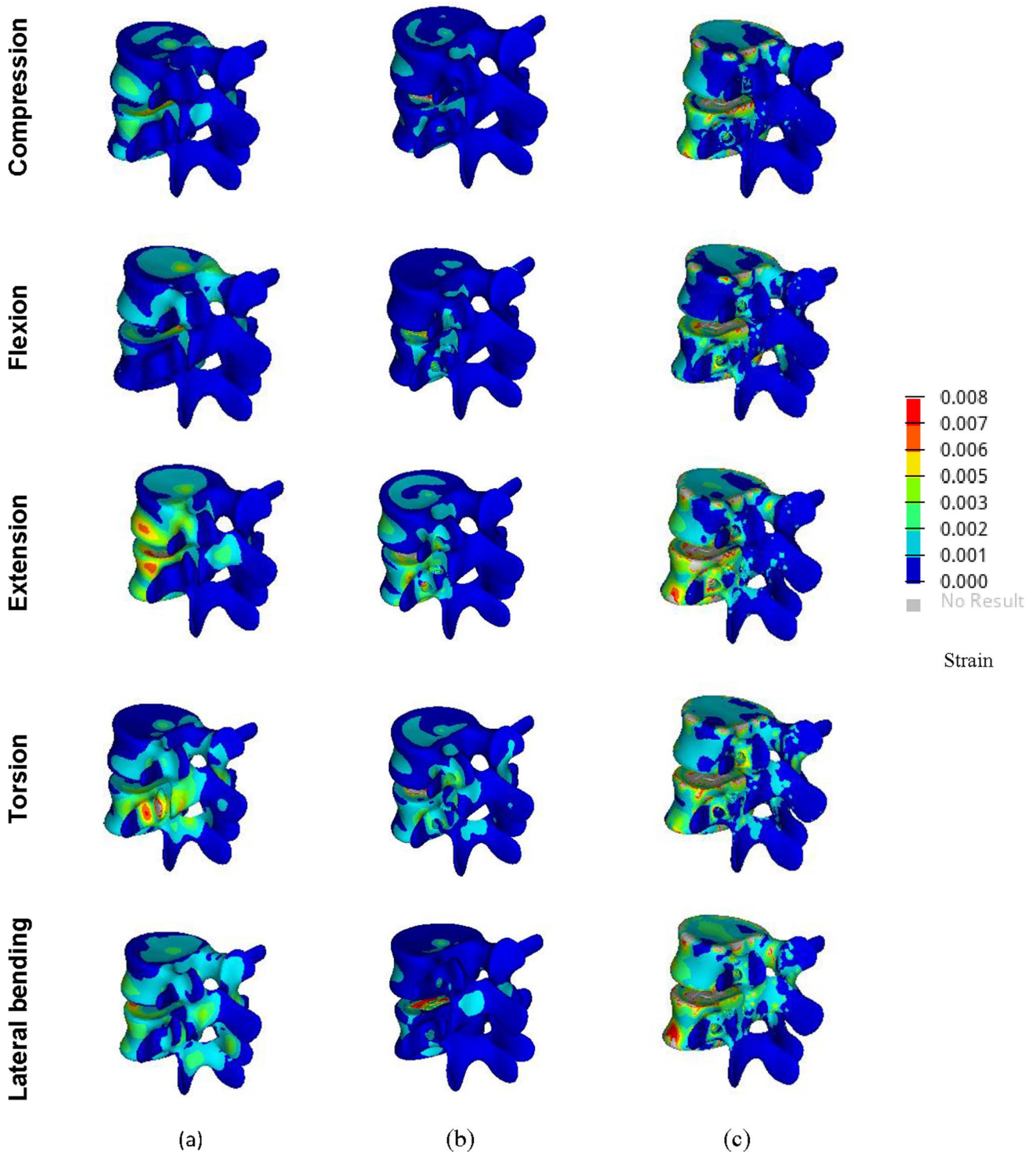


Fig. 10 Von-Mises strain contours in cancellous bone for (a) intact FSU and FSUs corresponding to (b) normal and (c) expandable pedicle screw, respectively

in the neck region of the screw for loading conditions, e.g. flexion, extension, lateral bending, and torsion. The stress distribution pattern in case of intact FSU was found to corroborate well with the predictions from Talukdar et al.

(2021) [40], whereas the value of highest maximum stress in cancellous bone was found to be quite in agreement with Xu et al. (2019) [46]. However, the peak stress was predicted across different locations, depending on the type of

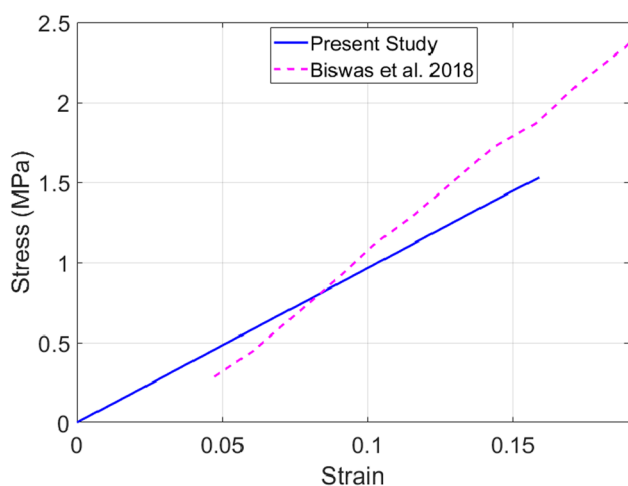


Fig. 11 Stress–strain diagram of intervertebral disc (IVD) in intact FSU under compression

load. While subjected to torsion, the peak stress was predicted on the posterior side of L5 vertebra though under lateral bending, it was found on the anterior side (Fig. 6a). It can, therefore, be inferred that under lateral bending, stress might be concentrated towards anterior side of the vertebrae. Under torsion, regions having high stress concentration were found to be less pronounced in L4 as compared to that under flexion or extension (Figs. 6a and 7a). This perhaps could be because the loading was more concentrated on L5 during torsion. Moreover, the stress concentration was more towards right side of L4 under flexion but on the left side under extension (Figs. 6a and 7a). This can be attributed to the direction of loading (moment).

The implantation of normal pedicle screws, expandable pedicle screws, and cage resulted in a significant change of stress contours (around 30–100%) for different loading conditions. Marginally greater stress shielding was predicted in case of the normal pedicle screw as opposed to expandable pedicle screw under all loading scenarios (Figs. 6b and c and 7b and c). The peak stress was found to be near base of pedicle screw in cortical bone for all load cases. The reason behind this was supposed to be due to high stress concentration near pedicle area. Apart from the peak stress region, the overall stress values were below 30 MPa for cases other than compression. It could also be noted that for cancellous bone the stress was higher near the cage insertion area for both normal and expandable pedicle screws (Figs. 7b and c and 8b and c).

Like stress, the strain distribution patterns for both cortical and cancellous bone were found to be influenced by the application of various loading condition. The equivalent (von-Mises) strain under compression was found to corroborate well with previous literatures [40, 70]. The peak strain was found to be the least under compression and the highest

under torsion for the intact L4–L5 vertebra (Fig. 9a). For intact model, the peak strain area was predicted towards posterior side of in L5 vertebra under torsion (Fig. 9a). However, the peak strain was found more towards anterior side under lateral bending (Figs. 9a and 10a). The peak strain area in L4 vertebra was found to be more in both flexion and extension than torsion (Figs. 9a and 10a). Following stress concentration pattern, strain was high towards right side under flexion but on the left side of L4 under extension (Figs. 9a and 10a) due to loading direction.

Under various physiological loading conditions, the instrumentation of both normal and expandable pedicle screws resulted in around 40–100% increase in peak strain field. The peak strain was found near screw insertion area in cortical bone (Fig. 9b and c) and near cage insertion area in cancellous bone (Fig. 10b and c). The peak strain was predicted to be the least under compression and the highest under extension in the implanted bones (Figs. 9b and c and 10b and c). Nonetheless, the peak strain values in the bone were found to be considerably higher in case of expandable pedicle screws.

It was estimated that fixation with expandable pedicle screw provided greater fixation strength in case of compromised bone. Compromised situation arises during osteoporosis or during revision surgery, and it was found that during those situations, expandable pedicle screw showed improved results in clinical studies [33]. Wu et al. (2010) [12] reported no failure/breakage of expandable pedicle screw. It was further concluded that expandable pedicle screw might have acted as valued tool for growth in armamentarium for spinal fixation [59]. Vertebra instrumented with expandable pedicle screws for patients with degenerative spinal deformity showed improved results in clinical as well as radiological outcomes with only 2.1% cases of screw pullout on larger stress sites [19]. The authors attributed this to the design of the expandable pedicle screw [19]. Marginally greater area (15–80%) with peak stresses at the bone–screw interfaces, as predicted in our present study, may elevate the risk of such pullout instances in expandable screw. It appears from the stress–strain contours that the expandable pedicle screw may result in lower loosening rate as compared to normal pedicle screw. However, greater stress concentration predicted at the screw insertion area in the former implant may also lead to pullout risk to a certain extent owing to interfacial debonding.

The stress–strain curve of IVD corresponding to intact FSU in the present study was found to be closely associated with the values reported in the literature [71] (Fig. 11). However, maximum stress in the IVD was reported to be 1.86 MPa by Biswas et al. [71], as opposed to 1.53 MPa in our study. This deviation may be attributed to some difference in loading and boundary conditions. Further, Biswas et al. [71] used stress–strain curve as an

input criterion for material properties. The reduced stress in the IVD in case of implanted models could be the result of more load transfer in the cage. The maximum stress in IVD was found to be the lowest in case of FSU instrumented with expandable pedicle screw. This suggests that the expandable pedicle screw exerted more stress shielding on IVD than the normal pedicle screws.

There were, however, certain limitations and assumptions made in the current study. Firstly, cancellous bone was considered as linear, elastic, and isotropic though cancellous bone is typically anisotropic in nature [72]. Moreover, muscles were not included in this study though muscle plays a significant role for lumbar spine stability [22, 52, 73]. The ligaments were considered to be tension-only elements for static load transfer [40, 52, 74]. The capsular ligament was not included [40]. It may further be noted that the load values may vary significantly depending on the body weight.

5 Conclusion

The expandable pedicle screw predicted marginally improved anchorage having greater contact area with the bones as compared to the normal pedicle screws. More contact area with the bone resulted in greater stresses at the contact sites indicative of better stability and load transfer to the bone. Nevertheless, this may lead to marginally greater risk of screw pullout. Greater area (15–80%) with peak stresses at the bone-screw interfaces also indicates lesser degree of stress shielding in case of the former implant. Thus, with the use of expandable pedicle screws, one may expect to have lower loosening issues. However, at IVD, 45% higher stress shielding was predicted with expandable screws. The various physiological loading regimes also appeared to have considerable influence on the overall load transfer in the L4-L5 vertebrae. However, peak stresses on cortical and cancellous bone were found to be clinically admissible for all cases. These predictions notwithstanding, in vitro and in vivo evaluations are presently being envisaged for further insights into these two implants.

Acknowledgements The authors would like to acknowledge the computational facilities available at the Biomechanics Laboratory of the Department of Biosciences and Bioengineering, Indian Institute of Technology Guwahati, which has helped carry out this study. The authors would like to thank Rahul Gautam Talukdar, PhD scholar, IIT Kharagpur for his valued help. The authors would also like to acknowledge Dr. Chandralekha Baruah, MD Radiodiagnosis, Senior Resident, Dr. Ram Manohar Lohia Hospital and ABVIMS, New Delhi, and Dr. Udit Chahal, MS Orthopedics, Fellow in Arthroplasty, Max Hospital, Mohali, for their valuable input. The study has been partially supported by SERB, India (Grant no. SRG/2019/000235).

Declarations

Conflict of interest The authors declare no competing interests.

References

1. Atlas SJ, Deyo RA (2001) Evaluating and managing acute low back pain in the primary care setting. *J Glob Inf Manag* 16:120–131. <https://doi.org/10.1111/j.1525-1497.2001.91141.x>
2. Keramat A, Larigani B, Adibi H (2012) Risk factors for spinal osteoporosis as compared with femoral osteoporosis in Urban Iranian women. *Iran J Public Health* 41(10):52–59
3. Zou D, Muheremu A, Sun Z et al (2020) Computed tomography Hounsfield unit-based prediction of pedicle screw loosening after surgery for degenerative lumbar spine disease. *J Neurosurg Spine* 32:716–721. <https://doi.org/10.3171/2019.11.SPINE19868>
4. Sivasubramaniam V, Patel HC, Ozdemir BA et al (2015) Trends in hospital admissions and surgical procedures for degenerative lumbar spine disease in England: a 15-year time-series study. *BMJ Open* 5:e009011. <https://doi.org/10.1136/bmjopen-2015-009011>
5. Yoganandan N, Kumaresan S, December PFA (2000) Geometric and mechanical properties of human cervical spine ligaments. *ASME J Biomech Eng* 122(6):623–629. <https://doi.org/10.1115/1.1322034>
6. Sanjay D, Kumar N, Chanda S (2021) Stress-strain distribution in intact L4–L5 vertebrae under the influence of physiological movements: a finite element (FE) investigation. *IOP Conf Ser Mater Sci Eng* 1206:012024. <https://doi.org/10.1088/1757-899X/1206/1/012024>
7. White III AA, Panjabi MM (1978). *Book-clinical biomechanics of the spine*
8. Kabins MB, Weinstein JN (1991) The history of vertebral and pedicle screw fixation. *The Iowa orthop j* 11:127–136
9. Li C, Zhou Y, Wang H et al (2014) Treatment of unstable thoracolumbar fractures through short segment pedicle screw fixation techniques using pedicle fixation at the level of the fracture: a finite element analysis. *PLoS ONE* 9(6):1–9. <https://doi.org/10.1371/journal.pone.0099156>
10. Wang T, Wu B, Duan R et al (2020) Treatment of thoracolumbar fractures through different short segment pedicle screw fixation techniques: a finite element analysis. *Orthop Surg* 12:601–608. <https://doi.org/10.1111/os.12643>
11. Moore DC, Maitra RS, Farjo LA et al (1997) Goldstein restoration of pedicle screw fixation with an in situ setting calcium phosphate cement. *Spine* 22(15):1696–1705. <https://doi.org/10.1097/00007632-199708010-00003>
12. Wu ZS, Cui G, Lei W et al (2010) Application of an expandable pedicle screw in the severe osteoporotic spine: a preliminary study. *The J. Clinic. Investig.* 33(6):368–374. <https://doi.org/10.25011/cim.v33i6.14587>
13. Glazer J, Starley M, Sayre H et al (2003) A 10-year follow up evaluation of lumbar spine fusion with pedicle screw fixation. *Spine* 28(13):1390–1395. <https://doi.org/10.1097/01.BRS.0000067112.15753.AD>
14. Moran JM, Berg WS, Berry JL et al (1989) Transpedicular screw fixation. *J. Orthop. Res.* 107-114. <https://doi.org/10.2147/mder.s3747>
15. Alizadeh M, Kadir MRA, Fadhli MM et al (2013) The use of X-shaped cross-link in posterior spinal constructs improves stability in thoracolumbar burst fracture: a finite element analysis. *J Orthop Res* 31(9):1447–1454. <https://doi.org/10.1002/jor.22376>
16. Liao JC, Chen WP, Wang H (2017) Treatment of thoracolumbar burst fractures by short-segment pedicle screw fixation

- using a combination of two additional pedicle screws and vertebroplasty at the level of the fracture: a finite element analysis. *BMC Musculoskelet Disord* 18(1):1–8. <https://doi.org/10.1186/s12891-017-1623-0>
17. Alanay A, Vyas R, Shamie AN et al (2007) Safety and efficacy of implant removal for patients with recurrent back pain after a failed degenerative lumbar spine surgery. *J Spinal Disord Tech* 20(4):271–277. <https://doi.org/10.1097/01.bsd.0000211283.14143.ad>
 18. Li Y, Cheng H, Liu ZC et al (2013) In vivo study of pedicle screw augmentation using bioactive glass in osteoporosis sheep. *J Spinal Disord Tech* 26(4):118–123. <https://doi.org/10.1097/BSD.0b013e31827695e2>
 19. Qi W, Yan Y, bo, Zhang Y, et al (2011) Study of stress distribution in pedicle screws along a continuum of diameters: a three-dimensional finite element analysis. *Orthop Surg* 3(1):57–63. <https://doi.org/10.1111/j.1757-7861.2010.00112.x>
 20. Viezens L, Sellenschloh PK et al (2021) Impact of screw diameter on pedicle screw fatigue strength- a biomechanical evaluation. *World Neurosurg* 152:369–376. <https://doi.org/10.1016/j.wneu.2021.05.108>
 21. Otsuki B, Fujibayashi S, Tanida S et al (2021) Possible association of pedicle screw diameter on pseudoarthrosis rate after transforaminal lumbar interbody fusion. *World Neurosurg* 150:e155–e161. <https://doi.org/10.1016/j.wneu.2021.02.117>
 22. Biswas J, Sahu TP, Rana M et al (2019) Design factors of lumbar pedicle screws under bending load: a finite element analysis. *Bio-cybern Biomed Eng* 39(1):52–62. <https://doi.org/10.1016/j.bbe.2018.10.003>
 23. Chen SI, Lin RM, Chang CH (2003) Biomechanical investigation of pedicle screw-vertebrae complex: a finite element approach using bonded and contact interface conditions. *MedEng Phys* 25(4):275–282. [https://doi.org/10.1016/S1350-4533\(02\)00219-9](https://doi.org/10.1016/S1350-4533(02)00219-9)
 24. Pearson HB, Dobbs CJ, Grantham E et al (2017) Intraoperative biomechanics of lumbar pedicle screw loosening following successful arthrodesis. *J Orthop Res* 35(12):2673–2681. <https://doi.org/10.1002/jor.23575>
 25. Cho W, Cho SK, Wu C (2010) The biomechanics of pedicle screw-based instrumentation. *J Bone Joint Surg* 92B:1061–1065. <https://doi.org/10.1302/0301-620X.92B8.24237>
 26. Halvorson TL, Kelley LA, Thomas KA et al (1994) Effect of bone mineral density on pedicle screw fixation. *Spine* 19(21):2415–2420. <https://doi.org/10.1097/00007632-199411000-00008>
 27. Paxinos O, Tsitsopoulos P, Zindrick MR et al (2010) Evaluation of pullout strength and failure mechanism of posterior instrumentation in normal and osteopenic thoracic vertebrae. *J. Neurosurg* 13(4):469–476. <https://doi.org/10.3171/2010.4.SPINE09764>
 28. Fu J, Yao ZM, Wang Z et al (2018) Surgical treatment of osteoporotic degenerative spinal deformity with expandable pedicle screw fixation: 2-year follow-up clinical study (2018). *Orthop Traumatol Surg Res* 104(3):411–415. <https://doi.org/10.1016/j.otsr.2017.11.010>
 29. Gazzeri R, Roperto R, Fiore C (2016) Surgical treatment of degenerative and traumatic spinal diseases with expandable screws in patients with osteoporosis: 2-year follow-up clinical study. *J Neurosurg Spine* 25(5):610–619. <https://doi.org/10.3171/2016.3.SPINE151294>
 30. Rahyussalim AJ, Kurniawati T, Besri NN et al (December) (2019) Osteoporotic pedicle screw: review of various types of pedicle screw and cement augmentation. *AIP Conf Proc* 2193. <https://doi.org/10.1063/1.5139323>
 31. Su KC, Chen KH, Pan CC et al (2021) Biomechanical evaluation of cortical bone trajectory fixation with traditional pedicle screw in the lumbar spine: a finite element study. *Appl Sci* 11(22):10583. <https://doi.org/10.3390/app112210583>
 32. Aebi M (2014) Revision and stabilisation surgery of an adult degenerative scoliosis. *Eur Spine* 23:703–705. <https://doi.org/10.1007/s00586-014-3224-z>
 33. Cook SD, Barbara J, Rubi M et al (2001) Lumbosacral fixation using expandable pedicle screws: an alternative in reoperation and osteoporosis. *Spine J* 1:109–114. [https://doi.org/10.1016/s1529-9430\(01\)00020-1](https://doi.org/10.1016/s1529-9430(01)00020-1)
 34. Cook SD, Salkeld SL, Whitecloud TS et al (2000) Biomechanical evaluation and preliminary clinical experience with an expansive pedicle screw design. *J Spinal Disord* 13:230–236. <https://doi.org/10.1097/00002517-200006000-00006>
 35. Weng F, Wang J, Yang L et al (2018) Application value of expansive pedicle screw in the lumbar short-segment fixation and fusion for osteoporosis patients. *Exp Ther Med* 16(2):665–670. <https://doi.org/10.3892/etm.2018.6248>
 36. Chanda S, Gupta S, Pratidhar DK (2016) Effect of interfacial conditions on shape optimization of cementless hip stem: an investigation based on a hybrid framework. *Struct Multidisc Optim* 53:1143–1155. <https://doi.org/10.1007/s00158-015-1382-1>
 37. Sahu NK, Kaviti AK (2016) A review of use of FEM techniques in modeling of human knee joint. *J. Biomimetics. Biomater Biomed Eng* 28:1–11. <https://doi.org/10.4028/www.scientific.net/JBBBE.28.14>
 38. Sanjay D, Mondal S, Bhutani R et al (2018) The effect of cement mantle thickness on strain energy density distribution and prediction of bone density changes around cemented acetabular component. *Proc IMechE Part H: J Engineering in Medicine* 232(9):912–921. <https://doi.org/10.1177/0954411918793448>
 39. Mondal S, Ghosh R (2019) Effects of implant orientation and implant material on tibia bone strain, implant-bone micromotion, contact pressure, and wear depth due to total ankle replacement. *Proc IMechE Part H: J Engineering in Medicine* 233(3):318–333. <https://doi.org/10.1177/0954411918823811>
 40. Talukdar RG, Mukhopadhyay KK, Dhara S et al (2021) Numerical analysis of the mechanical behaviour of intact and implanted lumbar functional spinal units: effects of loading and boundary conditions. *Proc IMechE Part H: J Engineering in Medicine* 235(7):792–804. <https://doi.org/10.1177/09544119211008343>
 41. Biswas JK, Malas A, Majumdar S et al (2022) A comparative finite element analysis of artificial intervertebral disc replacement and pedicle screw fixation of the lumbar spine. *Comput Methods Biomech Biomed Eng* 12:1–9. <https://doi.org/10.1080/10255842.2022.2039130>
 42. Dreischarf M, Zander T, Shirazi-Adl A et al (2014) Comparison of eight published static finite element models of the intact lumbar spine: predictive power of models improves when combined together. *J Biomech* 47(8):1757–1766. <https://doi.org/10.1016/j.jbiomech.2014.04.002>
 43. Ayturk UM, Puttlitz CM (2011) Parametric convergence sensitivity and validation of a finite element model of the human lumbar spine. *Comput Methods Biomech Biomed Eng* 14(8):695–705. <https://doi.org/10.1080/10255842.2010.493517>
 44. Kiapour A, Anderson DG, Spenciner DB et al (2012) Kinematic effects of a pedicle-lengthening osteotomy for the treatment of lumbar spinal stenosis Laboratory investigation. *J Neurosurg Spine* 17(4):314–320. <https://doi.org/10.3171/2012.6.SPINE11518>
 45. Rohlmann A, Lauterborn S, Dreischarf M et al (2013) Parameters influencing the outcome after total disc replacement at the lumbosacral junction. Part 1: misalignment of the vertebrae adjacent to a total disc replacement affects the facet joint and facet capsule forces in a probabilistic finite element analysis. *Eur Spine J* 22(10):2271–2278. <https://doi.org/10.1007/s00586-013-2909-z>
 46. Xu M, Yang J, Lieberman IH et al (2019) Finite element method-based study of pedicle screw–bone connection in pullout test and

- physiological spinal loads. *Med Eng Phys* 67:11–21. <https://doi.org/10.1016/j.medengphy.2019.03.004>
47. Xu M, Yang J, Lieberman IH et al (2016) Lumbar spine finite element model for healthy subjects: development and validation. *Comput Methods Biomech Biomed Eng* 20(1):1–15. <https://doi.org/10.1080/10255842.2016.1193596>
 48. Goel VK, Kiapour A, Faizan A et al (2007) Finite element study of matched paired posterior disc implant and dynamic stabilizer (360° motion preservation system). *SAS Journal* 1(1):55–62. [https://doi.org/10.1016/S1935-9810\(07\)70047-6](https://doi.org/10.1016/S1935-9810(07)70047-6)
 49. Zander T, Rohlmann A, Burra NK et al (2006) Effect of a posterior dynamic implant adjacent to a rigid spinal fixator. *Clin Biomech* 21(1):767–774. <https://doi.org/10.1016/j.clinbiomech.2006.04.001>
 50. Rohlmann A, Burra NK, Zander T et al (2007) Comparison of the effects of bilateral posterior dynamic and rigid fixation devices on the loads in the lumbar spine: a finite element analysis. *Eur Spine J* 16(8):1223–1231. <https://doi.org/10.1007/s00586-006-0292-8>
 51. Boccaccio A, Vena P, Gastaldi D et al (2008) Finite element analysis of cancellous bone failure in the vertebral body of healthy and osteoporotic subjects. *Proc IMechE Part H: J Engineering in Medicine* 222:1023–1036. <https://doi.org/10.1243/09544119JEIM296>
 52. Zhang Z, Lic H, Fogeld GR et al (2018) Finite element model predicts the biomechanical performance of transforaminal lumbar interbody fusion with various porous additive manufactured cages. *Comput Biol Med* 95:167–174. <https://doi.org/10.1016/j.compbiomed.2018.02.016>
 53. Kim K, Park WM, Kim YH et al (2010) Stress analysis in a pedicle screw fixation system with flexible rods in the lumbar spine. *Proc IMechE Part H: J Engineering in Medicine* 224(3):477–485. <https://doi.org/10.1243/09544119JEIM611>
 54. Song M, Sun K, Li Z et al (2021) (2021) Stress distribution of different lumbar posterior pedicle screw insertion techniques: a combination study of finite element analysis and biomechanical test. *Sci Rep* 11:12968. <https://doi.org/10.1038/s41598-021-90686-6>
 55. Ambati DV, Wright EK, Lehman RA et al (2015) Bilateral pedicle screw fixation provides superior biomechanical stability in transforaminal lumbar interbody fusion: a finite element study. *Spine* 15(8):1812–1822. <https://doi.org/10.1016/j.spinee.2014.06.015>
 56. Kim DH, Hwang RW, Lee GH et al (2020) Comparing rates of early pedicle screw loosening in posterolateral lumbar fusion with and without transforaminal lumbar interbody fusion. *Spine J* 20:1438–1445. <https://doi.org/10.1016/j.spinee.2020.04.021>
 57. Tai CL, Tsai TT, Lai PL et al (2015) A biomechanical comparison of expansive pedicle screws for severe osteoporosis: the effects of screw design and cement augmentation. *PLoS ONE* 10(12):e0146294. <https://doi.org/10.1371/journal.pone.0146294>
 58. Fisher C, Harty J, Yee A et al (2022) Perspective on the integration of optical sensing into orthopedic surgical devices. *J Biomed Opt* 27(1):010601. <https://doi.org/10.1117/1.JBO.2.7.1.010601>
 59. Gokhale NS, Deshpande SS, Bedekar SV, Thite AN (2008). *Book-practical finite element analysis*. 445
 60. Zhou Q, Zeng F, Tu J et al (2020) Influence of cement augmented pedicle screw instrumentation in an osteoporotic lumbosacral spine over the adjacent segments: a 3d finite element study. *J Orthop Surg Res* 15(1):132–(1–8). <https://doi.org/10.1186/s13018-020-01650-5>
 61. Wong CE, Hu HT, Kao LH et al (2022) Biomechanical feasibility of semi-rigid stabilization and semi-rigid lumbar interbody fusion: a finite element study. *BMC Musculoskelet Disord* 23:10. <https://doi.org/10.1186/s12891-021-04958-3>
 62. Li J, Shang J, Zhou Y et al (2015) Finite element analysis of a new pedicle screw-plate system for minimally invasive transforaminal lumbar interbody fusion. *PLoS ONE* 10(12):1–16. <https://doi.org/10.1371/journal.pone.0144637>
 63. Vena P, Franzoso G, Gastaldi D et al (2005) A finite element model of the L4–L5 spinal motion segment: biomechanical compatibility of an interspinous device. *Comput Methods Biomech Biomed Eng* 8(1):7–16. <https://doi.org/10.1080/1025584050062914>
 64. Xiao Z, Wang L, Gong H et al (2011) A non-linear finite element model of human L4–L5 lumbar spinal segment with three-dimensional solid element ligaments. *Theor App Mech Lett* 1(6):064001–(1–6). <https://doi.org/10.1063/2.1106401>
 65. Markolf KL (1972) Deformation of the thoracolumbar intervertebral joints in response to external loads: a biomechanical study using autopsy material. *J Bone Joint Surg* 54(3):511–533
 66. Jain P, Khan MR (2022) Comparison of novel stabilisation device with various stabilisation approaches: a finite element based biomechanical analysis. *Int J Artif Organs*. <https://doi.org/10.1177/03913988221088334>
 67. Yamamoto I, Panjabi MM, Crisco T et al (1989) Three-dimensional movements of the whole lumbar spine and lumbosacral joint. *Spine* 14(11):1256–1260. <https://doi.org/10.1097/0007-632-198911000-00020>
 68. Zhong ZC, Wei SH, Wang JP et al (2006) Finite element analysis of the lumbar spine with a new cage using a topology optimization method. *Med Eng Phys* 28:90–98. <https://doi.org/10.1016/j.medengphy.2005.03.007>
 69. Chen CS, Cheng CK, Liu CL et al (2001) Stress analysis of the disc adjacent to interbody fusion in lumbar spine. *Med Eng Phys* 23(7):483–491. [https://doi.org/10.1016/s1350-4533\(01\)00076-5](https://doi.org/10.1016/s1350-4533(01)00076-5)
 70. Morgan EF, Bayraktar HH, Keaveny TM (2003) Trabecular bone modulus-density relationships depend on anatomic site. *J Biomech* 36(7):897–904. [https://doi.org/10.1016/s0021-9290\(03\)00071-x](https://doi.org/10.1016/s0021-9290(03)00071-x)
 71. Biswas JK, Rana M, Roy S et al (2018) Effect of range of motion (ROM) for pedicle screw fixation on lumbar spine with rigid and semi-rigid rod materials: a finite element study. *IOP Conf Ser Mater Sci Eng* 402:012146. <https://doi.org/10.1088/1757-899X/402/1/012146>
 72. Wolframa U, Wilke HJ, Zysset PK (2010) Valid μ finite element models of vertebral trabecular bone can be obtained using tissue properties measured with nanoindentation under wet conditions. *J Biomech* 43(9):1731–1737. <https://doi.org/10.1016/j.jbiomech.2010.02.026>
 73. Chiang MF, Zhong ZC, Chen CS et al (2006) Biomechanical Comparison of Instrumented Posterior Lumbar Interbody Fusion With One or Two Cages by Finite Element Analysis. *Spine* 31(19):682–689. <https://doi.org/10.1097/01.brs.0000232714.72699.8e>
 74. Zhong ZC, Chen SH, Hung CH (2008) Load and displacement-controlled finite element analyses on fusion and non-fusion spinal implants. *Proc IMechE Part H: J Engineering in Medicine* 223(2):143–157. <https://doi.org/10.1243/09544119JEIM476>

Publisher's note Springer Nature remains neutral with regard to jurisdictional claims in published maps and institutional affiliations.



Devismita Sanjay Ms. Devismita Sanjay did her Master's in Machine Design in 2015. She worked as a junior research fellow in IIT Mandi, India from Dec 2016 till Jul 2018. Ms. Sanjay joined the Department of Biosciences and Bioengineering at IIT Guwahati as a doctoral scholar in Dec. 2018. Her broad areas of research interest include spine biomechanics and implant design.



Neeraj Kumar Mr. Neeraj Kumar has worked as a research fellow in two defence research laboratories of India from 2016 to 2020 after completing his Bachelor's in mechanical engineering. Subsequently, he joined the Department of Biosciences and Bioengineering at IIT Guwahati, India as a Jr. Research Fellow. His broad areas of research interest include FE analysis and computational mechanics.



Jaideep Singh Bhardwaj Mr. Jaideep Singh Bhardwaj received his Master's with distinction in Biotechnology in the year 2020. He is presently a doctoral scholar in the Department of Biosciences and Bioengineering at IIT Guwahati, India. His research interests include biomechanics, implant design, in vitro testing, and 3D printing.



Souptick Chanda Dr. Souptick Chanda, Ph.D. is a Fulbright fellow who is presently working as an Assistant Professor in the Department of Biosciences and Bioengineering at IIT Guwahati, India. His areas of research interest include biomechanics, implant design and optimization, surgical simulations, and soft computing.